Skylight polarization during a total solar eclipse: a quantitative model

G. P. Können

Royal Netherlands Meteorological Institute, P.O. Box 201, 3730 AE De Bilt, The Netherlands

Received April 23, 1986; accepted October 9, 1986

The polarization distribution in the sky during a total solar eclipse is calculated with a simple secondary light-scattering model. This model uses the light-intensity measurements near the horizon during the eclipse and the pretotality and posttotality skylight polarization observations as input. It is found that the model can explain various observations during totality, including the quantitative measurements of Shaw [Appl. Opt. **14**, 388 (1975)] of the polarization distribution of the sky in the solar vertical during the 1973 total eclipse.

1. INTRODUCTION

When the totality phase of a solar eclipse starts, the appearance of the sky changes dramatically. In a rapid transition the circumstances change from full daylight to a situation comparable to twilight, which is accompanied by a sudden drop in the sky intensity of about 3 orders of magnitude.[1–3] The remaining lighting of the sky is caused by multiple scattering of sunlight, which starts in the region outside the lunar umbra,[3] instead of by singly scattered light from a well-defined point source during nontotality conditions. (The light of the solar corona is 6 orders of magnitude weaker than that of the uneclipsed Sun[3] and therefore makes only a negligible contribution to the illumination.) Therefore the illumination of the sky during totality must be described basically in a two-step process: (1) at least one scattering in the region outside the umbra, followed by some absorption; and (2) at least one scattering inside the umbra.[4] Light resulting from the first step is visible during totality as a reddish band about 10° in width above the horizon all around us; this band acts as the light source for the illumination of the sky above us. Above 10–20°, light from the two-step process dominates the scenery.[5]

Since the polarization for singly scattered light and multiply scattered light differs completely, the polarization pattern of the sky also changes abruptly at totality. It has been known since at least 1905 (Ref. 6) that the polarization of the sky decreases drastically, at least at 90° from the Sun. Starting in 1961, a few instrumental records have been published of the polarization change of the sky during eclipses.[7–11] However, the information obtained by these early observers about this state of polarization of the sky is rather limited, since they restricted their measurements to one single point in the sky, located at 90° from the Sun in the solar vertical. This situation lasted until 1973, when Shaw recorded the polarization of the sky as a function of the zenith angle during the June 30th eclipse.[1] He found a symmetry in the polarization with respect to the zenith, with a minimum value in the zenith and maximum polarization rather close to the horizon. His data are complete enough to justify the development of a simple model as a first attempt to come to a quantitative understanding of the polarization of the sky during solar eclipses.

In this perspective, we present in this paper a simple two-step scattering model for the polarization of the sky during totality. It is based on secondary scattering by a degraded Rayleigh scatterer in which the depolarization factor is deduced from the pretotality and posttotality measurements, and it uses the observed intensity distribution near the horizon during totality as input. Despite the simplicity of this approach, its numerical results compare satisfactorily with observations made during various eclipses.

2. FORMULATION OF THE MODEL

The propositions of the model are the following:

1. The polarization is described as result of a two-step scattering process.
2. Step 1 is the scattering of sunlight in a region outside the umbra, followed by some absorption and depolarization and possibly by additional scattering by aerosols.
3. In the numerical evaluations, the polarization of light resulting from step 1 must be neglected, since the available data do not include measurements of it.
4. Step 2 is single scattering to the observer of light produced in step 1 by a degraded Rayleigh scatterer.
5. The paths of light from step 1 to the secondary scattering centers are parallel to the ground.
6. The secondary scattering centers are close to the observer.
7. The scattering matrix $\mathcal{M}$ of step 2 is identical to the scattering matrix during pretotality and posttotality and is given by a linear combination of a pure Rayleigh scatterer and an unpolarized isotropic scatterer.[12]

Some comments must be made on the above-mentioned propositions and the handling of them.

a. Light resulting from step 1 is concentrated near the horizon. Its intensity is taken from the observations.
b. The depolarization factor of the degraded Rayleigh scatterer is taken from the pretotality and posttotality skylight polarization observations.

0740-3232/87/030601-08$02.00

c. Neglect of polarization resulting from step 1 is justified if the optical thickness along the line between the observer and the edge of the umbra is large enough. In that case additional scatterings by aerosols are important, and they destroy the polarization. This depolarization can be expected to be more effective at small wavelengths. As we will see below, there is some indirect evidence for this depolarization in Shaw's 400-nm measurements. In Appendix A, a quantitative estimate is made from the effect of relaxing proposition 3 and hence introducing polarization in step 1.

d. It should be noted that the propositions of our model are close to the ones used by Soret[13] and by Ahlgrimm[14] in their models to describe the polarization of sunlit sky, taking into account secondary scattering.

e. The validity of the model is restricted to the regions of the sky where single scattering can be neglected, i.e., above a height of about 20° over the horizon.[5]

3. CALCULATION OF THE POLARIZATION DISTRIBUTION

Since circularly polarized light does not show up in the two-step process, we can describe the polarization of light by a three-dimensional Stokes vector **S**:

$$\mathbf{S} = \begin{bmatrix} I \\ Q \\ U \end{bmatrix} \equiv \begin{bmatrix} I \\ IP\cos 2\phi \\ IP\sin 2\phi \end{bmatrix}. \tag{1}$$

Here I denotes the intensity, P denotes the degree of polarization, and ϕ denotes the angle of polarization with respect to a plane of reference.[15,16] We take the vertical as the plane of reference for Stokes vectors **S**. However, for scattering matrices $\mathcal{M}$, the scattering plane is taken to be the plane of reference. Let $\mathbf{S}_1$ be the Stokes vector of light after step 1, thus entering the secondary scattering center from the horizon, and let $\mathcal{T}(\phi)$ be the rotation matrix defined by

$$\mathcal{T}(\phi) = \begin{bmatrix} 1 & 0 & 0 \\ 0 & \cos 2\phi & \sin 2\phi \\ 0 & -\sin 2\phi & \cos 2\phi \end{bmatrix}. \tag{2}$$

The Stokes vector $\mathbf{S}_2$ after step 2 is then found by the matrix multiplication[16]

$$\mathbf{S}_2 = \mathcal{T}(-\phi_3)\mathcal{M}\mathcal{T}(\phi_2)\mathbf{S}_1. \tag{3}$$

Here ϕ_2 denotes the angle of the scattering plane with the vertical in step 2 as seen from the secondary scattering center in the direction of the light ray incoming from the horizon, and ϕ_3 denotes the angle of this scattering plane with the vertical as seen by the observer looking to the secondary scattering center.

From proposition 7, the scattering matrix is given by[12,16]

$$\mathcal{M} = \begin{bmatrix} 1+\cos^2\theta + I_D & -\sin^2\theta & 0 \\ -\sin^2\theta & 1+\cos^2\theta & 0 \\ 0 & 0 & 2\cos\theta \end{bmatrix}, \tag{4}$$

where the factor I_D results from the unpolarized isotropic scattering matrix and θ denotes the scattering angle. A substitution of this matrix $\mathcal{M}$ into Eq. (3) yields the Stokes vector $\mathbf{S}_2$ in arbitrary units, as normalization constants have been omitted in Eq. (4).

In pretotality and posttotality, single scattering is dominating, and $\mathcal{M}$ is acting on $\mathbf{S}_0 = (1, 0, 0)$. When this matrix multiplication is carried out for single scattering, the degree of polarization becomes

$$P \equiv \frac{\sqrt{Q^2+U^2}}{I} = \frac{\sin^2\theta}{1+\cos^2\theta + I_D}, \tag{5}$$

which gives, for $\theta = 90°$,

$$P = \frac{1}{1+I_D}. \tag{6}$$

So, with the aid of Eq. (5) or (6), the factor I_D in Eq. (4) that determines the degradation with respect to pure Rayleigh scattering can be fixed from measurements outside totality.

The evaluation of the two-step process with Eq. (3) requires the introduction of some angles. We define z as the solar elevation, h as the height in the sky where the observer is looking (height of the secondary scattering center), ψ as the azimuth of the secondary scattering center minus the azimuth of the Sun, α as the azimuth of a light ray coming in to the secondary center and measured relative to the line connecting the observer with secondary scattering center, and ψ_1 as the azimuth of a light ray coming in to the secondary center minus the azimuth of the Sun.

All angles ψ_1, ψ, α, ϕ_2, ϕ_3 are taken to be positive in the anticlockwise direction. Under proposition 6, the relation

$$\psi_1 = \psi + \alpha \tag{7}$$

holds. Figure 1 displays the geometry of the problem.

The Stokes vector $\mathbf{S}_1$ is a function of ψ_1 and depends on several factors, among them the distance to the edge of the umbra, the cloud decks, and the reflectivity of the Earth. If we assume the latter two factors to be constant around the observer, $\mathbf{S}_1$ will be a symmetrical function of ψ_1 during midtotality. Relaxing proposition 3 for a moment, $\mathbf{S}_1$ can be expressed as

$$\mathbf{S}_1 = \mathcal{T}(-\phi_1)\mathcal{M}'\mathbf{S}_0 f(\psi_1), \tag{8}$$

in which $\mathcal{M}'$ is given by Eq. (4) with an unknown factor I_D' in it, ϕ_1 is the angle of the primary scattering plane relative to the vertical, $f(\psi_1)$ is the azimuthal dependence of $\mathbf{S}_1$ after integration of all primary scattering centers in the direction ψ_1 outside the umbra, and $\mathbf{S}_0 = (1, 0, 0)$ is the Stokes vector of the Sun. Note that the factorization of $\mathbf{S}_1$ in Eq. (8) in a matrix multiplication and an azimuth-dependent intensity function $f(\psi_1)$ acting equally on all Stokes parameters is an approximation, one that is completely true if step 1 contains just a single scattering.

From spherical geometry one finds the relations

$$\cos\theta_1 = \cos z \cos\psi_1$$

and

$$\tan\phi_1 = -\sin\psi_1/\tan z, \tag{9}$$

where θ_1 denotes the scattering angle in step 1.

A straightforward calculation of the intensity function

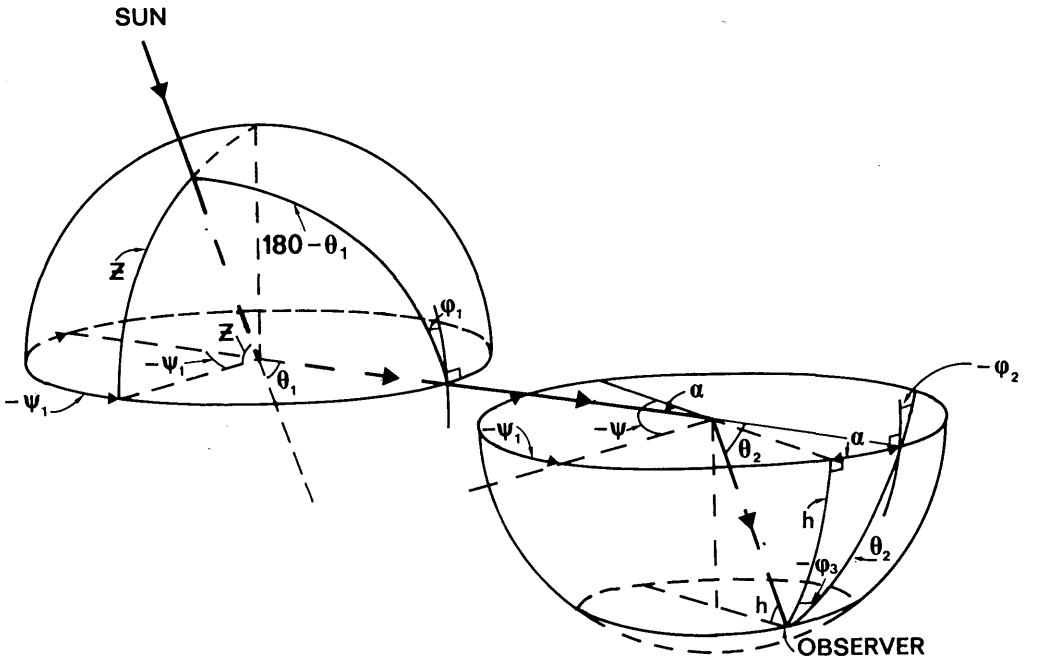

Fig. 1. Geometry of the two-step scattering model. The definitions of the angles are given in the text.

$f(\psi_1)$ from the geometry of the umbra is permitted only for an optically thin atmosphere and for homogeneous meteorological conditions and surface reflectivity around the observation site. If we neglect the extinction and the curvature of the Earth,[5] we get simply

$$f(\psi_1) \propto r^{-1}(\psi_1), \tag{10}$$

where r denotes the distance of the observer from the edge of the umbra (r is not too small). Of course, the shape of the umbra is an ellipse. Hence, if the observer is the central point of this ellipse, one finds from Eq. (10) that

$$f(\psi_1) = (1 - \cos^2 z \cos^2 \psi_1)^{1/2} \simeq 1 - \tfrac{1}{2} \cos^2 z \cos^2 \psi_1. \tag{11}$$

The latter approximation holds if $\cos^2 z$ is not too large. When the observer is in one of the foci of the ellipse, one finds that

$$f(\psi_1) = 1 + \cos z \cos \psi_1. \tag{12}$$

When the optical thickness along r is sufficiently large, $f(\psi_1)$ may deviate from expression (10). This will be more likely if the wavelength is shorter. However, a decrease of $f(\psi_1)$ with increasing r can be expected anyhow. For this case, we use instead of expression (11) the approximate expression

$$f(\psi_1) = 1 - a^2 \cos^2 \psi_1, \tag{13}$$

where the empirical factor $a^2 < 1$ is determined from the intensity measurements near the horizon during eclipse. Because of the uncertainty in the processes in step 1 (among them the depolarization that is due to processes such as small-angle scattering), such an empirical approach should always be preferred for the determination of $\mathbf{S}_1$ above a direct calculation from Eq. (8).

Under proposition 3, one has, with Eq. (7), for $\mathbf{S}_1$

$$\mathbf{S}_1 = \begin{bmatrix} f(\psi + \alpha) \\ 0 \\ 0 \end{bmatrix}. \tag{14}$$

Furthermore, one finds from spherical geometry for step 2 the following expressions from Fig. 1:

$$\begin{aligned} \cos \theta_2 &= \cos \alpha \cos h, \\ \tan \phi_2 &= -\sin \alpha / \tan h, \\ \tan \phi_3 &= -\tan \alpha / \sin h. \end{aligned} \tag{15}$$

Here, θ_2 is the scattering angle in step 2.

Carrying out Eq. (3) leads to the following expressions for the Stokes parameters in $\mathbf{S}_2$:

$$\begin{aligned} I_2(h, \psi, \alpha) &= (1 + I_D + \cos^2 h \cos^2 \alpha) f(\psi + \alpha), \\ Q_2(h, \psi, \alpha) &= (1 - [1 + \sin^2 h] \cos^2 \alpha) f(\psi + \alpha), \\ U_2(h, \psi, \alpha) &= \sin 2\alpha \sin h f(\psi + \alpha). \end{aligned} \tag{16}$$

Integration of Eqs. (16) over α from $0 \rightarrow 2\pi$ yields the desired Stokes vector at (h, ψ) in the sky. We denote this end result by a barred symbol $\bar{\mathbf{S}}_2 = (\bar{I}_2, \bar{Q}_2, \bar{U}_2)$. Equations (16) imply that the relation

$$\bar{\mathbf{S}}_2(h, \psi) = \bar{\mathbf{S}}_2(h, \psi + 180°) \tag{17}$$

holds. Thus, in a given vertical plane, the polarization at either side of the zenith is equal.

To calculate $\bar{\mathbf{S}}_2$, we first take the intensity function $f(\psi_1)$ of the form of Eq. (12) (the observer is at one of the foci of the ellipse-shaped umbra). Integration of Eqs. (16) then yields

$$\bar{I}_2(h, \psi) = \pi[2(1 + I_D) + \cos^2 h],$$
$$\bar{Q}_2(h, \psi) = \pi \cos^2 h,$$
$$\bar{U}_2(h, \psi) = 0, \tag{18}$$

which shows that the direction of the plane of polarization is always vertical ($\bar{Q}_2 > 0$, $\bar{U}_2 = 0$) and the degree of polarization P is independent of the azimuth and independent of the ellipticity of the umbra and hence of z. Therefore the degree of polarization becomes essentially the same as for a circularly shaped umbra and is given by

$$P(h, \psi) = \frac{\bar{Q}_2}{\bar{I}_2} = \frac{\cos^2 h}{2(1 + I_D) + \cos^2 h}, \tag{19}$$

which ranges from zero in zenith to maximally 33% near horizon. If one applies Eq. (13) for $f(\psi_1)$ (midtotality and the observer at the central line of eclipse), one has

$$\bar{I}_2(h, \psi) = \pi[(2 - a^2)(1 + I_D) + (1 - \tfrac{1}{4}a^2 \cos 2\psi - \tfrac{1}{2}a^2)\cos^2 h]$$
$$\bar{Q}_2(h, \psi) = \pi[\tfrac{1}{2}a^2 \cos 2\psi + (1 - \tfrac{1}{4}a^2 \cos 2\psi - \tfrac{1}{2}a^2)\cos^2 h]$$
$$\bar{U}_2(h, \psi) = \tfrac{1}{2}\pi a^2 \sin 2\psi \sin h, \tag{20}$$

which remains azimuth dependent. In the solar vertical ($\psi = 0, 180°$), $\bar{U}_2 = 0$ and $\bar{Q}_2 > 0$, so that the polarization is vertical again. The degree of polarization is given by

$$P(h, 0) = P(h, 180°) = \frac{\bar{Q}_2(h, 0)}{\bar{I}_2(h, 0)}$$
$$= \frac{\tfrac{1}{2}a^2 + (1 - \tfrac{3}{4}a^2)\cos^2 h}{(2 - a^2)(1 + I_D) + (1 - \tfrac{3}{4}a^2)\cos^2 h}. \tag{21}$$

In the plane perpendicular to the solar vertical containing the zenith ($\psi = 90°, 270°$), $\bar{U}_2$ is zero again, but $\bar{Q}_2$ changes sign at

$$\cos^2 h_n = \frac{2a^2}{4 - a^2}, \tag{22}$$

indicating the existence of neutral points at either side of the solar vertical during mideclipse. Since $a^2 < 1$, these neutral points will always be higher in the sky than 35°.

If the observer is not in the center of the umbra anymore, or if $f(\psi_1)$ is otherwise irregularly distributed around the observer, then $\bar{U}_2(h, 0)$ may be nonzero. This indicates some tilt in the direction of polarization. However, Eqs. (16) indicate that $\bar{U}_2(h, 0)$ is usually much closer to zero than is $\bar{Q}_2(h, 0)$ if the properties of $f(\psi_1)$ are not too extreme. Therefore the model does not yield much change in the direction of polarization in the solar vertical when the eclipse proceeds. Of course, if proposition 3 is relaxed, larger tilts of the polarization plane become possible.

4. COMPARISON WITH OBSERVATIONS

A. Polarization Distribution in the Solar Vertical

The only measurements of the polarization distribution in the sky that have come to our attention are those taken by Shaw during the 1973 eclipse.[1] He scanned during totality the degree of polarization in the solar vertical as a function of the zenith angle for a wavelength of 400 nm (presented in his Fig. 10). At the same wavelength he measured the degree of polarization as a function of time for a fixed point in the sky, chosen in the solar vertical and at 90° from the Sun (his Fig. 9). Moreover, he performed intensity scans at 400 and 600 nm in the solar vertical and in the plane perpendicular to it (his Figs. 2–5).

Although it can be inferred from his Figs. 9 and 10 that his polarization scan in the solar vertical did not take place at midtotality, it is not possible to reconstruct its exact timing. For this reason, and because the intensity scans in Figs. 2 and 4 of Ref. 1 provide only a few points of the radiance during the eclipse near the horizon (necessary input for our model), it is also not possible to give an exact experimental value for the intensity function $f(\psi_1)$ in Eq. (14) after step 1, although it is obvious from Shaw's measurements that $f(\psi_1)$ changed during the course of the eclipse.

Fortunately, however, Shaw observed for 400 nm only a weak dependence of the intensity as a function of ψ_1. Therefore, it is possible to choose for $f(\psi_1)$ the simple form of formula (13). If we take for the intensity after step 1 the measured intensity at $h = 10°$ as the standard, we find that $a^2 = 0.1$. This is considerably less than the value of $a^2 = 0.3$, expected from geometry alone [formulas (10) and (11)]. This low value of a^2 can be considered an indication that proposition 3 is largely fulfilled at 400 nm. From Shaw's pretotality and posttotality measurements at 90° from the Sun, one finds that the degree of polarization without eclipse would have been 42%, and hence $I_D = 1.22$ [Eq. (6)].

Figure 2 compares Shaw's observations with the theory, Eq. (21). The agreement at $h > 25°$ is satisfactory, although our model generates a slightly lower polarization. However, from his time series, Shaw reported at midtotality a polarization of only 4% at 90° from the Sun, as compared with 9% during his solar vertical scan. So, rather than giving an underestimate, our model slightly overestimates the polarization, but such small differences are well within the uncertainties of the model results.

The experimental curve of Shaw shows some asymmetry with respect to the zenith, which Shaw attributes to differences in surface albedo around the observing site. However, our model predicts for every intensity function $f(\psi_1)$ a symmetric behavior of the polarization with respect to the zenith [see Eq. (17)], while during Shaw's eclipse proposition 3 seems to be largely fulfilled. Therefore we attribute the observed asymmetry chiefly to the change of the eclipse geometry and hence of $f(\psi_1)$ during the scan, taking into account that this scan would probably have taken at least 60 sec, i.e., 20% or more of the time of totality, and that the eclipse geometry is rapidly changing.

B. Direction of Polarization

In the solar vertical our model predicts at midtotality a vertical polarization. Unfortunately, Shaw did not present measurements of the angle of polarization. Therefore, at my request, Jannink[17] observed visually the direction of skylight polarization with the aid of a simple Minnaert polariscope[18] during the 1981 Siberian eclipse ($z = 25°$) near the Sun (so $h = 25°$). The observed direction of the easily visible polarization was within 10° of vertical. This visual observation was completed by a set of two slides that he

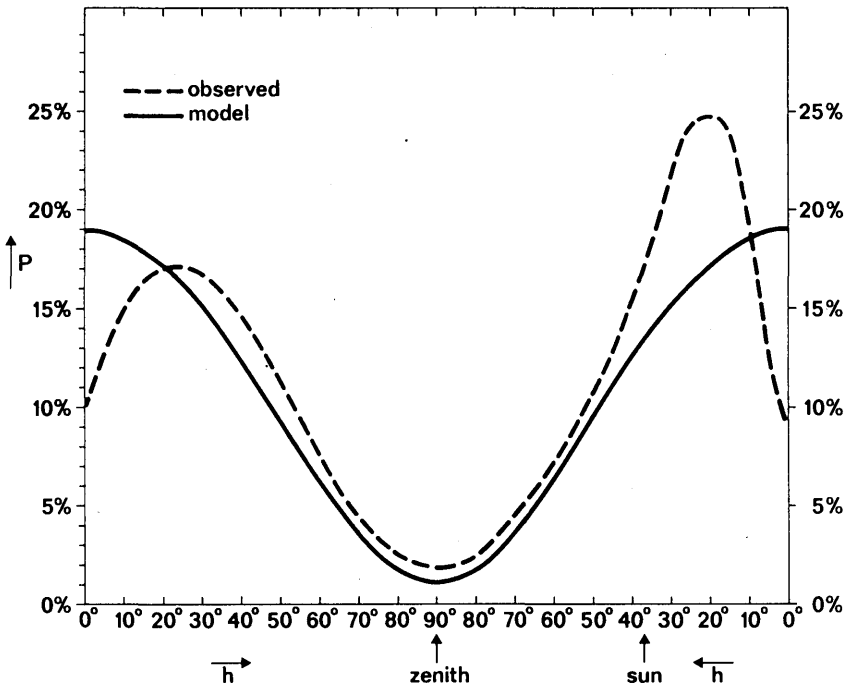

Fig. 2. Polarization distribution in the solar vertical during totality. The dashed line is the observed polarization reported by Shaw.[1] The solid line is the calculated polarization of the present two-step scattering model with parameters $I_D = 1.22$ and $a^2 = 0.1$, taken from Shaw's pretotality, posttotality, and intensity observations. Note that the model is essentially unable to describe the behavior for low h, where singly scattered light becomes dominant.

made with a polarizer before the camera (horizontal and vertical axes, respectively), showing both the polarization of the solar corona and that of the sky around it. The combination of these two data (together with the known shape of the corona during that particular eclipse) independently confirms his visual observation. From this report we conclude that in general the dominating aspect of the direction of polarization is vertical during eclipse, in agreement with our model.

By combining Jannink's observations with the measurements of Shaw, a further conclusion can be drawn on the applicability of the present theory. Since singly scattered light arriving in the solar vertical is horizontally polarized, a switch in the direction of polarization is expected at some height in the sky where multiple scattering starts to dominate. This switch should be accompanied by a local minimum of the degree of polarization as a function of height. However, in Shaw's scan no trace of such a minimum is apparent. This can be considered a second indication that for Shaw's observations the optical thickness is so large at 400 nm that light coming from outside the umbra is largely depolarized by additional (forward) scatterings in its path to the observer (comment c in Section 2). Again, this means that the application of our model with proposition 3 (neglecting the polarization of S_1) is justified for Shaw's observational conditions.

If one assumes that only light from step 2 is responsible for the polarization observed by Shaw at $h = 0$ (so $U_1 = Q_1 = 0$), and if one accepts our model result that the Stokes parameters after step 2 are weakly dependent on h for low h [see Eqs. (16), (18), and (20)], then it is possible to infer from the drop in the polarization near the horizon the relative intensities of light from step 1 and light from step 2. The decrease in the polarization by a factor of 2 between $h = 20°$ and $h = 0°$ indicates that near the horizon these intensities at 400 nm are of comparable strength, which is consistent with the outcomes of the various intensity scans of Shaw and which does not conflict with the theoretical findings of Gedzelman.[5]

C. Other Observations

Apart from Shaw's measurements, there are a few instrumental observations of the polarization of the sky during eclipses.[7-11] All the measurements have in common that they are made of a single fixed place in the sky, located in the solar vertical and at 90° from the Sun. Scans as a function of time have been reported, from which the value at maximum eclipse can be deduced. Since intensity scans near the horizon are not reported by these authors and the eclipse and observing conditions are different for each eclipse, a detailed comparison with theory cannot be carried out. However, to get an impression of it we have developed the following procedure. First, as a standard polarization distribution, we adopt the azimuth-independent polarization distribution given by Eq. (19) with $I_D = 1$. Second, each observed degree of polarization at mideclipse P_{tot} is transformed to P_{red}, which is the degree of polarization that would have been observed if $I_D = 1$ (which means that the observed degree of polarization at noneclipse conditions P_{pret} is replaced by a standard value of 0.5). This is done with aid of Eq. (19), so that

$$P_{red} = \frac{2(1 + I_D) + \cos^2 h}{4 + \cos^2 h} P_{tot} = \frac{2P_{pret}^{-1} + \cos^2 h}{4 + \cos^2 h} P_{tot}. \quad (23)$$

The values of P_{red} obtained in this way are compared with

Table 1. Summary of Instrumental Observations of Skylight Polarization at Mideclipse[a]

Observer(s)	Observation Number	Year	Wavelength (nm)	h (°)	P_{pret} (%)	P_{tot} (%)	P_{red} (%)
de Bary *et al.*[7]	1	1961	green	78	78	0	0
Moore and Rao[8]	2	1965	475	49	46	0.5	0.5
	3	1965	601	49	33	4.5	6.6
Miller and Fastie[9]	4	1965	558	25	62	31	26.0
	5	1965	578	25	66	35	28.0
	6	1965	610	25	49	28	28.5
	7	1965	630	25	47	26	27.4
Rao *et al.*[10]	8	1966	475	20	60.5	19	16.3
	9	1966	601	20	62.5	21	17.6
Dandekar and Turtle[11]	10	1970	475	44	42	4	4.7
	11	1970	600	44	42	<0.5	<0.6
Shaw[1]	12	1973	400	53	45	4	4.4

[a] P_{pret} is the polarization at noneclipse conditions (obtained from interpolation of the pretotality and posttotality measurements), P_{tot} is the polarization at mideclipse, and h is the height above the horizon of the point of observation. Since all measurements are performed in the solar vertical at 90° from the Sun, the solar elevation z can be found from $z = 90° - h$. P_{red} is the degree of polarization during eclipse after transformation to standard circumstances with $P_{pret} = 50\%$ ($I_D = 1$; see the text). The numbering corresponds to that in Fig. 3.

the standard polarization curve, which is Eq. (19) with $I_D = 1$.

Table 1 summarizes the observations (including that of Shaw), and Fig. 3 compares P_{red} with the standard curve. Although this method is quite rough, and the observations are done at very different conditions (e.g., observations 2–9 are from a high-flying aircraft), there is clearly a correlation between the curve and the observations, although the ground-based observations systematically yield a lower degree of polarization than does the theory (the same holds in principle for Shaw's polarization distribution, as outlined above). As shown in Appendix A, such behavior is to be expected if the polarization of light resulting from step 1 is completely neglected.

A few further remarks must be made. In the solar vertical, our model predicts essentially a vertical polarization during mideclipse. Moore and Rao,[8] however, reported for red a reversed polarization (their observation for blue is in agreement with our model). We attribute this effect to the larger contribution of polarization in S_1 for red light, which

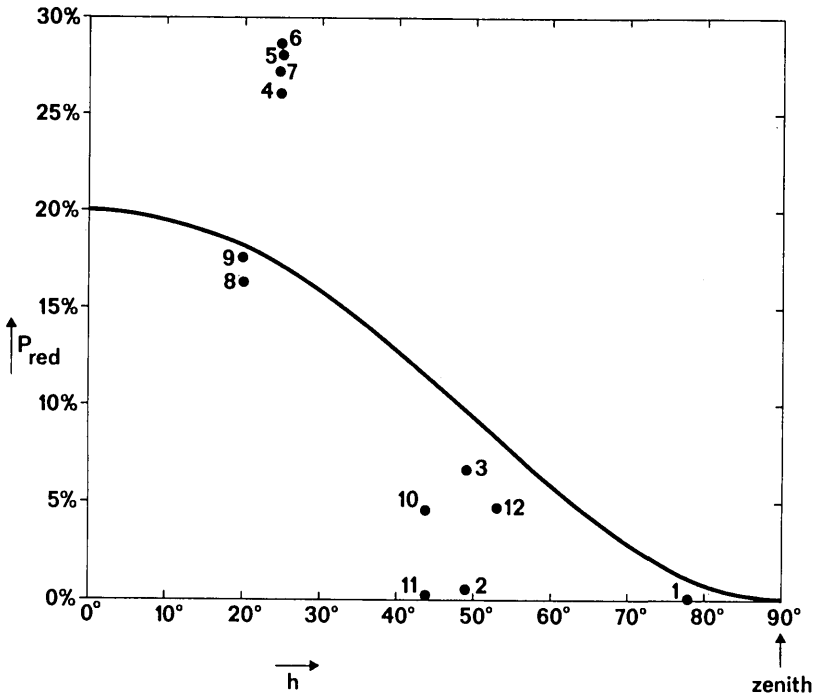

Fig. 3. Comparison of the observed degree of polarization during several eclipses with the theory. The observations are transformed into a degree of polarization P_{red} for standard circumstances. The theoretical curve is Eq. (19) with $I_D = 1$. The numbers at the points correspond to those in Table 1.

should result in a reduction of the vertical polarization of the sky (see Appendix A). The fact that Shaw's intensity measurements near the horizon at 600 nm largely satisfy expression (10) is consistent with this explanation. Furthermore, the polarization phase scan of Dandekar and Turtle[11] also displays a wavelength dependence. The fact that their measurements do not show a complete reversal of the polarization plane may be attributed to the eclipse geometry [the shape of $f(\psi_1)$], combined with a relatively large contribution of polarization in $\mathbf{S}_1$.

5. CONCLUSION

The previous section indicates that, despite its simplicity, our model seems to be able to describe the observations of the polarization of the sky during eclipses at least qualitatively and, in the case of Shaw's observations, even more than that. The conclusion might be drawn that, at least for the shorter wavelengths, it is justified to postpone propositions 1–7. For longer wavelengths, the analysis indicates that proposition 3 is the weakest of the propositions. The analysis in Appendix A indicates that our model with proposition 3 would overestimate the polarization for many solar heights; this finding is consistent with Subsection 4.C.

What remains to be discussed is the good agreement between Shaw's observations and the theory (Subsection 4.A). In the light of the findings in Appendix A, one may even wonder how far this close agreement is a lucky coincidence, caused by the short wavelength and by the fact that at $z = 37°$ the model is rather insensitive to the neglect of polarization of $\mathbf{S}_1$. Anyhow, one would expect at best only qualitative agreement if one calculates the polarization in this way from the limited data of $\mathbf{S}_1$. The close agreement was therefore also a surprise to us.

Within the limited set of existing observations there is no possibility to test the model further at present. This has to wait until more detailed observations are available. Such observations should include the polarization distribution of the eclipsed sky, preferably in the solar vertical plane and in the plane perpendicular to the solar vertical containing the zenith, together with simultaneous alumcanter scans of intensity and polarization near the horizon, all of them preferbly at various wavelengths. Only if such a complete set of measurements is available will a rigorous test of models like the present one be possible.

APPENDIX A: ANALYSIS OF THE EFFECT OF RELAXING PROPOSITION 3

To get an impression of the effect of proposition 3 (neglecting the polarization of $\mathbf{S}_1$), we calculate in the solar vertical for $h = 0$ and $h = 90°$ the polarization of the sky with and without proposition 3. The calculation is carried out explicitly for the special case in which the observer is located in the central point of a circularly shaped umbra, $f(\psi_1) = 1$. We note, however, that for an ellipse-shaped umbra the results are identical if the observer is at one of the foci of the ellipse.

In this appendix we maintain our notation, but for the model without proposition 3 a prime is added to the relevant symbols. Thus $P'(h)$ is the degree of polarization without proposition 3, $P(h)$ is the degree of polarization with proposition 3, and so on. In the present analysis, we take $I_D = 1$ in the scattering matrix $\mathcal{M}$ for step 2, as we did also in the standard curve used in Subsection 4.C.

If the Stokes vector after step 1 is given by $\mathbf{S}_1' = (I_1', Q_1', U_1')$, then the matrix multiplication of Eq. (3) results in

$$\mathbf{S}_2'(h = 90°) = \begin{bmatrix} 2I_1' - Q_1' \\ (-I_1' + Q_1')\cos 2\alpha \\ (I_1' - Q_1')\sin 2\alpha \end{bmatrix}, \tag{A1}$$

$$\mathbf{S}_2'(h = 0°) = \begin{bmatrix} I_1'(2 + \cos^2\alpha) + Q_1' \sin^2\alpha \\ Q_1'(1 + \cos^2\alpha) + I_1' \sin^2\alpha \\ 2U_1' \cos\alpha \end{bmatrix}, \tag{A2}$$

in which the solar vertical plane is the reference. By using Eqs. (8) and (9), $\mathbf{S}_1'$ can be specified. To make the results comparable to those obtained with Eq. (19), we use for step 1 a simplified scattering matrix $\mathcal{M}'$ in which the matrix element $m_{11}' = 1 + I_D'$ instead of $m_{11}' = 1 + I_D' + \cos^2\theta$. I_D' (the measure of depolarization in step 1) remains unspecified for the moment. For $f(\psi_1) = 1$, we have, from Eqs. (8) and (9),

$$\mathbf{S}_1' = \begin{bmatrix} I_1' \\ Q_1' \\ U_1' \end{bmatrix} = \begin{bmatrix} 1 + I_D' \\ \cos 2z - \cos^2\alpha \cos^2 z \\ \sin\alpha \sin 2z \end{bmatrix}. \tag{A3}$$

By substituting Eq. (A3) into Eqs. (A1) and (A2), one finds that after integration over α the third Stokes parameter in $\bar{\mathbf{S}}_2'$ is zero again for $h = 0°$ and $h = 90°$. The degree of polarization can be calculated from the integration of I_2' and Q_2' over α and results in

$$P'(h = 90°) = \frac{-\frac{1}{2}\cos^2 z}{4(1 + I_D') - 3\cos^2 z + 2}, \tag{A4}$$

$$P'(h = 0°) = \frac{(1 + I_D') + \frac{17}{4}\cos^2 z - 3}{5(1 + I_D') + \frac{7}{4}\cos^2 z - 1}. \tag{A5}$$

Here the sign of P' corresponds to that of $\bar{Q}_2'$. Thus $P' > 0$ means that the direction of polarization is parallel to the solar vertical plane. Under proposition 3, $Q_1 = U_1 = 0$ and we have $P = 0$ and $\frac{1}{5}$ for $h = 90°$ and $0°$, respectively. By taking now a lower limit of 1 for I_D', one has for $h = 90°$

$$0 < P(90°) - P'(90°) < 0.07\cos^2 z, \tag{A6}$$

indicating that proposition 3 tends to overestimate the polarization in the zenith by at the most a few percent [for Shaw's eclipse, $P(90°) - P'(90°) < 0.04$; for de Bary's[7] eclipse, $P(90°) - P'(90°) < 0.07$; and for Moore's[8] and Dandekar's[11] eclipses, $P(90°) - P'(90°) < 0.03$].

For $h = 0$, one has, from Eq. (A5) and $P(0°) = \frac{1}{5}$,

$$P(0°) - P'(0°) = \frac{\frac{14}{5} - \frac{39}{10}\cos^2 z}{5(1 + I_D') + \frac{7}{4}\cos^2 z - 1}, \tag{A7}$$

which indicates that for solar elevations below 32°, the introduction of proposition 3 tends to cause underestimation of the polarization. In the set of available observations (Table 1) none represents this case with low z but observation near the horizon. For $z > 32°$, Eq. (A7) indicates that assumption 3 causes overestimation of the polarization. If $I_D' > 1$, the upper limit of this overestimation ranges from 0.03 and

0.05 for the eclipses observed by Shaw[1] and Moore and Rao,[8] respectively, to 0.25 for those observed by Rao *et al.*[10] and by Miller and Fastie.[9]

REFERENCES

1. G. E. Shaw, "Sky brightness and polarization during the 1973 African eclipse," Appl. Opt. **14,** 388–394 (1975).
2. W. E. Sharp, S. M. Silverman, and J. W. F. Lloyd, "Summary of sky brightness measurements during eclipses of the sun," Appl. Opt. **10,** 1207–1210 (1971).
3. S. M. Silverman and E. G. Mullen, "Sky brightness during eclipses: a review," Appl. Opt. **14,** 2838–2843 (1975).
4. G. E. Shaw, "Sky radiance during a total solar eclipse: a theoretical model," Appl. Opt. **17,** 272–276 (1978).
5. S. D. Gedzelman, "Sky color near the horizon during a total solar eclipse," Appl. Opt. **14,** 2831–2837 (1975).
6. N. Piltschikoff, "Sur la polarisation du ciel pendant les éclipses du soleil," C. R. Acad. Sci. Paris **142,** 1449 (1906).
7. E. de Bary, K. Bullrich, and D. Lorenz, "Messungen der Himmelsstrahlung und deren Polarisationgrad während der Sonnenfinsternis am 15.2.1961 in Viareggio (Italien)," Geofis. Pura Appl. **48,** 193–198 (1961).
8. J. G. Moore and C. R. N. Rao, "Polarization of the daytime sky during the total solar eclipse of 30 May 1965," Ann. Geophys. **22,** 147–150 (1966).
9. R. E. Miller and W. G. Fastie, "Skylight intensity, polarization and airglow measurements during the total solar eclipse of 30 May 1965," J. Atmos. Terr. Phys. **34,** 1541–1546 (1972).
10. C. R. N. Rao, T. Takashima, and J. G. Moore, "Polarimetry of the daytime sky during solar eclipses," J. Atmos. Terr. Phys. **34,** 573–576 (1972).
11. B. S. Dandekar and J. P. Turtle, "Day sky brightness and polarization during the total eclipse of 7 March 1970," Appl. Opt. **10,** 1220–1224 (1971).
12. H. C. van de Hulst, *Multiple Light Scattering, Tables, Formulas and Applications,* Vol. 2 (Academic, New York, 1980).
13. J. L. Soret, "Sur la polarisation atmosphérique," Ann. Chim. Phys. **14,** 503–541 (1888).
14. F. Ahlgrimm, "Zur Theorie der atmosphärischen Polarisation," Jahrb. Hamburger Wiss. Anst. **32,** 1–66 (1914).
15. K. Serkowski, "Polarimeters for optical astronomy," in T. Gehrels, *Planets, Stars and Nebula, Studied with Photopolarimetry* (University of Arizona, Tucson, Ariz., 1974), pp. 135–174.
16. E. Collet, "The description of polarization in classical physics," Am. J. Phys. **36,** 713–725 (1968).
17. D. W. Jannink, Royal Netherlands Meteorological Institute, De Bilt, The Netherlands (personal communication, 1981).
18. G. P. Können, *Polarized Light in Nature* (Cambridge U. Press, Cambridge, 1985).